Circuit: Jurnal Ilmiah Pendidikan Teknik Elektro
Volume 8 No. 2 March 2024 - August 2024
ISSN: 2549-3698; E-ISSN: 2549-3701
DOI: 10.22373/crc.v8i2.19662

The Analysis and Mitigation of Harmonics Transformer Distribution at PT. PLN Syiah Kuala

Faisal[a], Ichsan Muhadis Lubis[a], Ghina Inayati[a], Tarmizi[a]

[a] Universitas Syiah Kuala, Indonesia

E-mail: Faisal1@mhs.unsyiah.ac.id

Submission: 18-08-2023 Accepted: 02-01-2024 Published: 01-08-2024

Abstract

In the event that there is a disturbance in the distribution of energy, the distribution transformer's function is to distribute electricity to customers. High harmonics are typically the source of issues in distribution transformers. The distribution transformer at PT. PLN (Persero) ULP Syiah Kuala has two issues: the neutral cable breaking and the main or secondary winding burning. Analyzing harmonics in distribution transformers at PT PLN (Persero) ULP Syiah Kuala is the goal of this study. The goal of this study is to measure, examine, and assess the transformers at Syiah Kuala ULP in order to select the best mitigation. One transformer had harmonic values that did not meet standards, according to the measurement results, and these values required to be reduced by combining passive filters. The results of THDi reduction using a passive filter yielded values for each phase R, S, and T of 4.79 %, 4.47%, and 4.69%, and these values are in accordance with the established standards. From the results of harmonic mitigation using a passive filter, the results obtained in accordance with the THDv and THDi standards based on IEEE 159-2014 are 8% and 10%, respectively.

Keywords*: Transformer, Harmonic, THD, Passive Filter*

Abstrak

Transformator distribusi bertujuan menyalurkan listrik ke pelanggan apabila terjadi gangguan distribusi listrik. Gangguan trafo distribusi biasanya disebabkan oleh harmonisa tinggi. Permasalahan yang terjadi pada trafo distribusi di PT.PLN (Persero) ULP Syiah Kuala adalah terbakarnya lilitan primer atau sekunder dan putusnya kabel netral. Penelitian ini bertujuan untuk menganalisis harmonisa pada trafo distribusi di PT.PLN (Persero) ULP Syiah Kuala. Penelitian ini untuk mengukur dan menganalisa dan mengukur trafo yang ada di ULP Syiah Kuala dan memilih mitigasi yang tepat. Dari hasil pengukuran diperoleh satu buah trafo yang memiliki nilai harmonisa yang tidak sesuai standar dan perlu dimitigasi dengan menggunakan kombinasi filter pasif. Dari hasil mitigasi harmonisa menggunakan filter pasif diperoleh hasil sesuai dengan standar THDv dan THDi. Berdasarkan IEEE 159-2014 masing-masing adalah 8% dan 10% dimana hasil reduksi THDi menggunakan filter pasif diperoleh nilai pada masing-masing phasa R,S dan T adalah 4.79%, 4.47% dan 4.69% dan nilai ini sudah sesuai dengan standar yang ditetapkan.

Kata kunci*:* Trafo, Harmonik, THD, Filter Pasif

Introduction

PT. PLN ULP Syiah Kuala is a government-owned enterprise operating in the electricity industry. This business separated from PLN ULP Merduati in order to provide better customer service. PLN ULP Syiah Kuala has 96,852 customers, where

customers served by PLN ULP Syiah Kuala come from the Banda Aceh City area including Kuta Alam District, Syiah Kuala District, Ulee Kareng District, and Aceh Besar District includes Babussalam District, Darussalam District, Krueng Barona Jaya District, Kuta Baro District, and Masjid Raya District. With an average monthly power sold of 26.1 million kwh, PLN ULP Syiah Kuala is able to produce an average of 27.8 million kwh per month. The Alue Naga feeder, the Hajj Dormitory feeder, the Beurawe feeder, the Cot Irie feeder, the Darussalam feeder, the SUTM City feeder, and the Kuta alam Lambhuk feeder are the 22 feeders at ULP Syiah Kuala. With 864 distribution transformer units dispersed throughout each feeder, the Lamdinding, Lamgugob, Lamnyong, Lamprit, Lamreung, Lingke, Neuheun, Peunayong, Prada, Syiah Kuala, Tanjong Selamat, Tungkop, Ujong Bate, and Ulee Kareng feeders are all type C feeders.

Transformers are used to scale up or step down voltage in power distribution to PLN ULP Syiah Kuala customers. However, damage to these transformers frequently arises, typically in the form of burned transformer windings, broken neutral wires, and blown fuses. Transformer winding burnout can result from internal short circuit and overload. Because of the high current flowing through it, resistance between the phases may result in a break in the neutral wire. The disconnection may not work if there is a disturbed short circuit. Total harmonic distortion, or THD, is a measure of how much harmonic content is present in a deformed wave. If a sine wave is distorted—that is, not in the shape of a natural sine—then it is said to include harmonics. THDv and THDi are both 0% in pure sine waves; standard THDv and THDi, as per IEEE 159-2014, are 8% and 10%, respectively [1]. Damage to a transformer caused by harmonics includes internal short circuits, heat-induced damage to the transformer's insulation, and damage to the neutral line.

Literature Review

a. Harmonics

According to Robert D. Henderson (1994), harmonics are a sinusoidal component of periodic waves with frequencies that are integral multiples of the fundamental frequency. Each periodic wave's frequency spectrum can be broken down into a number of component frequencies, such as the fundamental and harmonic component frequencies, for analysis. Periodic waves are represented by the following Fourier series in trigonometry:

$$V_o(t) = a_o + \sum_{n=1}^{\infty} \left(a_n \cos(n\omega t) + b_n \sin(n\omega t) \right) \quad \text{..... 1)}$$

Harmonics will appear if a sine wave is distorted, with Fourier analysis the distorted wave can be broken down (separated) into several sine waves as shown in Figure 1. The total voltage of the distorted sine wave as shown in Figure 1a can be broken down into fundamental waves (vs1) and harmonic waves (Vsh) as in Figure 1b and in the form of a harmonic spectrum in Figure 1.

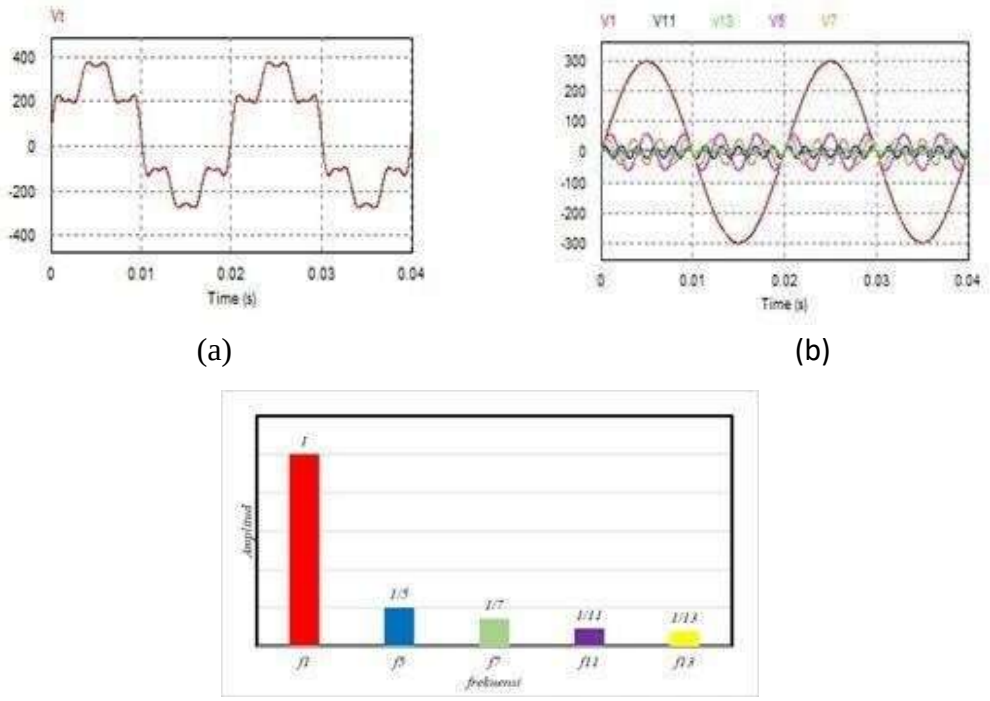

(a) (b)

(c)

Figure 1. 3-Phase System Harmonics, (a) Distorted Sine Wave of 3 Phase System; (b) 3-Phase Periodic Wave, (c) 3-Phase Harmonic Spectrum

The total stress equation is written as the following equation:

$$v_s(t) = v_{s1}(t) + \sum_{h=1}^{\infty} v_{sh}(t)$$
$$= \sqrt{2}V_{s1}\sin(\omega_1 t - \varphi_1) + \sum_{h=1}^{\infty} \sqrt{2}V_{sh}\sin(\omega_h t - \varphi_h)$$

where :

vs1(t) = Voltage at the fundamental frequency
vsh(t) = Harmonic current component
Vs1 = Fundamental rms voltage
Vsh = Rms harmonic voltage component
Vsh = Rms harmonic voltage component

The total harmonic voltage content of THDv (total harmonic distortion) is:

$$THD_v = \frac{\sqrt{\sum_{h=1}^{\infty} V_{sh}^2}}{V_{S1}} x100\%$$

While the total content of THDi harmonic currents is:

$$THD_i = \frac{\sqrt{\sum_{h=1}^{\infty} I_{sh}^2}}{I_{S1}} x100\%$$

Where:

Vsh = 2nd, 3rd, 4th, 5th harmonic component of voltage
Ish = Current harmonic component to 2,3,4,5...etc
Vs1 = Fundamental voltage component (50Hz)
Is1 = Fundamental current component (50Hz)

The relationship between THD and power factor (PF) is:

$$PF = \frac{P}{S} = \frac{V_s I_{s1} \cos\varphi_1}{V_s I_s} = \frac{I_{s1}}{I_s}\cos\varphi_1 = \frac{I_{s1}}{I_s} DPF = \frac{1}{\sqrt{1+THD_i^2}} DPF$$

b. Passive Power Filter

Passive power filters work based on the principle of a resonance circuit, the resonant frequency is tuned (set by the capacitor and inductor values) at a certain hiermonic order frequency value as shown in Figure 2.

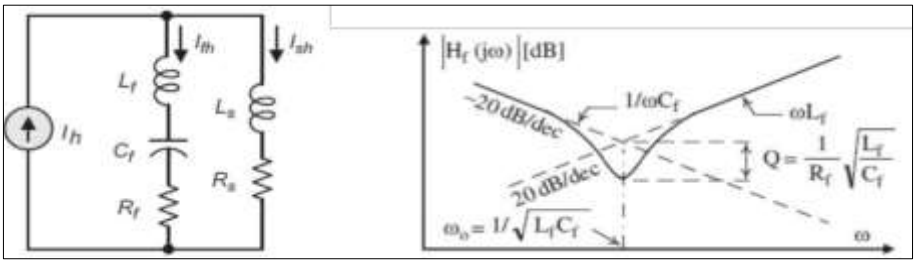

Figure 2. Resonance (a) circuit (b) response

Parallel passive filters (Shunt passive tuned) consist of several types namely, single tuned, double tuned, triple tuned with a series capacitor and triple tuned with a series inductor, the shape of the circuit is as shown in Figure 3.

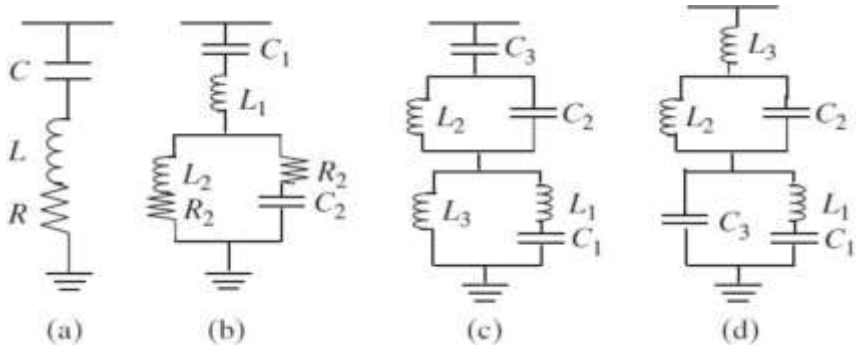

Figure 3. Shunt passive tuned (a), single tuned (b), double tuned (c), triple tuned (d)

Method

In carrying out the analysis and mitigation of harmonics in the distribution transformer, the steps shown are as shown in the flowchart in the following figure.

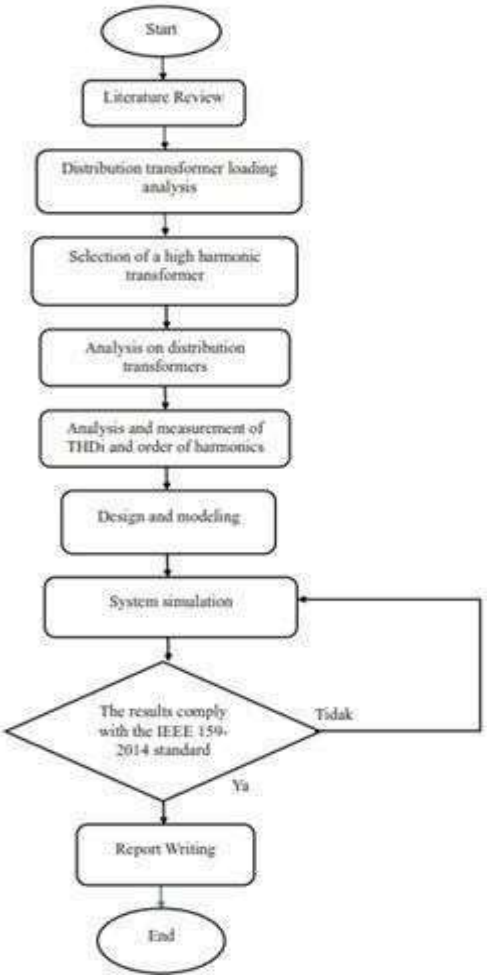

Figure 4. Flowchart of Research Implementation

Starting with Figure 4, where the research flow will be executed step-by-step. In order to get the intended outcome, the research steps need to be completed in order. Each study step is explained in the following points:

a. Literature Review

Research on distribution systems, distribution transformers, harmonics, and their effects on the electrical system—particularly distribution systems—began at the outset of this activity. A number of papers on these topics were reviewed and studied. Next, ascertain where the measurement is being taken. Distribution transformer harmonics are measured at the feeder, which is disrupted the most frequently. The repeaters at ULP Syiah Kuala include the Alue Naga feeders, the Hajj Dormitory feeders, the Beurawe feeders, the Cot Irie feeders, the Darussalam feeders, the SUTM City feeders, the Kuta alam feeders Lambhuk feeders, the Lamdinding feeders, the Lamgugob feeders, the Lamnyong feeders, the Lamprit feeders, the Lambhuk feeders. Lamreung, Lingke krc feeder, Neuheun krc feeder, Peunayong feeder, Prada krc feeder, Syiah Kuala feeder, Tanjong Selamat feeder, Tungkop feeder, Ujong Bate feeder and Ulee Kareng feeder. Out of the 22 feeders and 864 distribution transformer units, one feeder—the Lamnyong feeder—was chosen as it frequently caused disruptions and damage to the distribution lines and transformers. Next, measurements are made in accordance with the Transformer in Lamnyong Feeder Single Line Diagram, which looks like this.

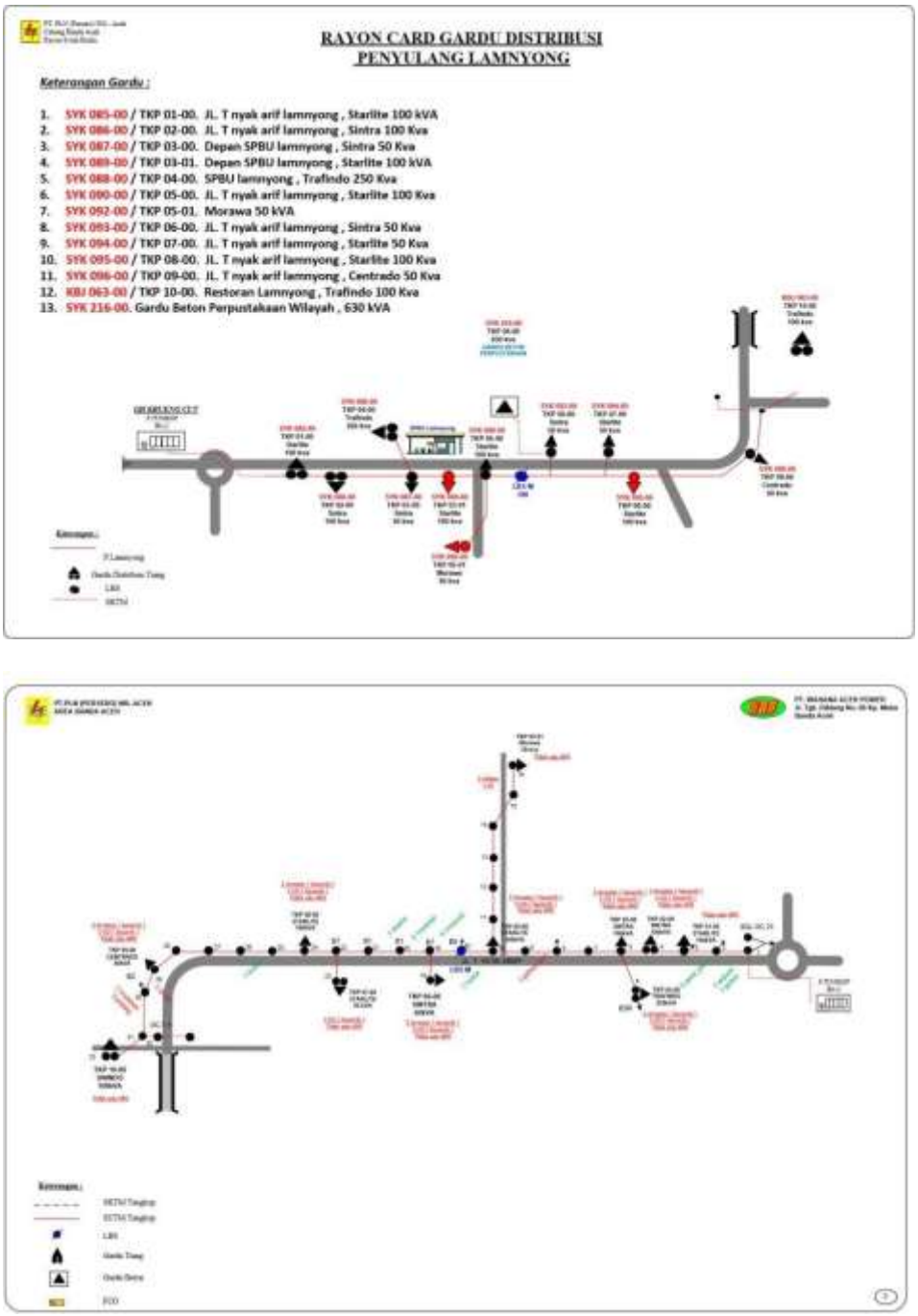

Figure 5. Single Line Diagram of the ULP Syiah Kuala Lamnyong Feeder

b. Analysing Distribution Transformer Loading

To make it easier to choose a transformer with high harmonics, an analysis of distribution transformer measurements is conducted. This includes understanding the frequency, voltage, and current values of the transformer to determine the size of the load sustained by the transformer. From Figure 5 it can be seen that measurements can be made on 11 existing transformers in Feeder Lamnyong. After measuring the 11 transformers, the results obtained after the measurements are as follows.

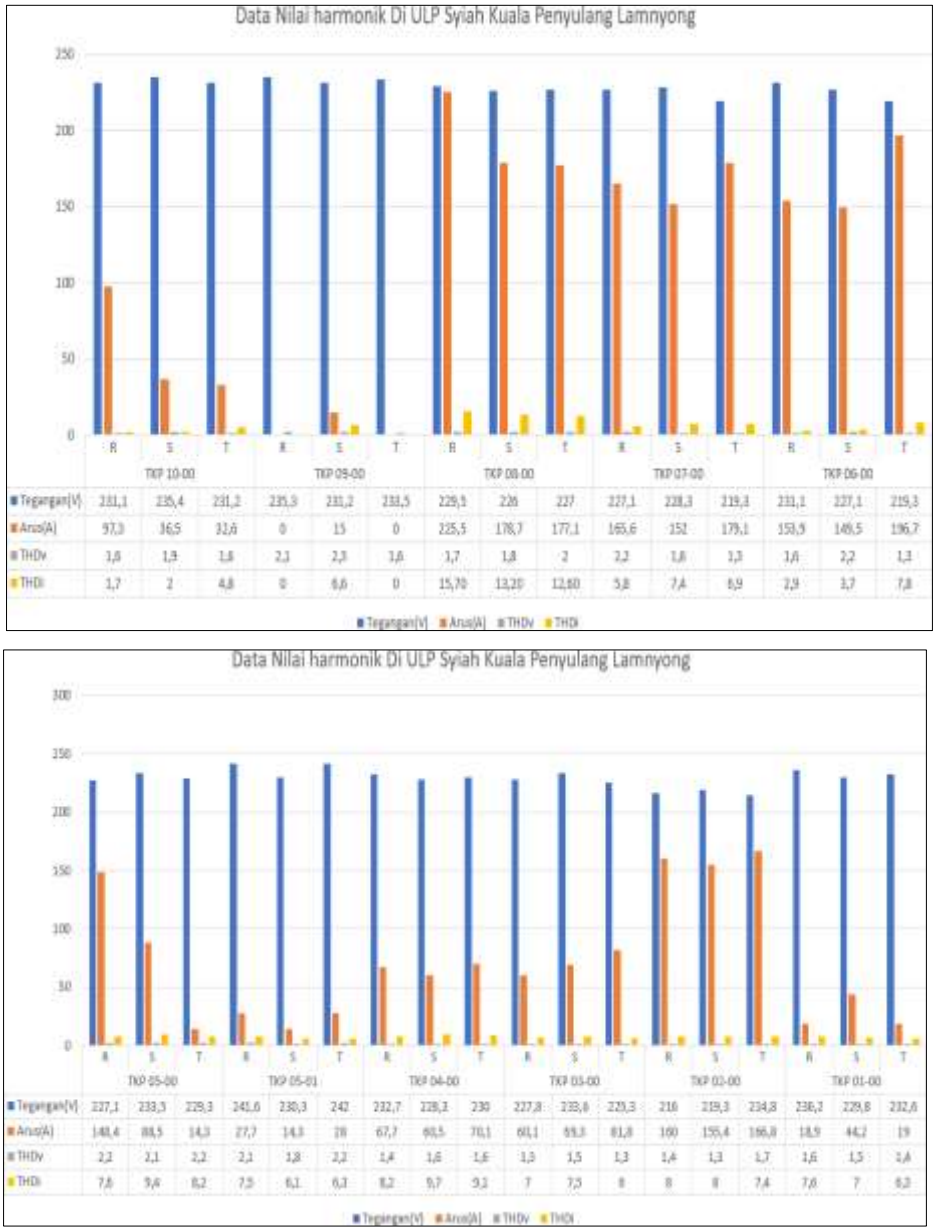

Figure 6. Results of Harmonic Measurements on the ULP Syiah Kuala Sulang LamnyongTransformer

Based on the measurement results, it is evident that a number of transformers require mitigation in order to lower the harmonics present in them and comply with IEEE 159-2014's THDv and THDi requirements, which are 10% and 8%, respectively. Based on Figure 6, it can be seen that there are current THD and voltage THD data. THDv is indicated in gray and THDi is indicated in yellow. In Figure 6 there are 11 transformers that are measured where there are results of THDv and THDi measurements on each of the R, S and T phases. From these data it can be seen that there are transformers that have high harmonics. Meanwhile, the THDv value contained in the image does not exceed the IEEE 159-2014 standard limit, namely the THDv standard limit of 8%. The THDv value in the image has a THD value that is almost the same, while the THDi value has a variety of values.

c. Selection of High Harmonic Transformer

In order to lower the harmonics, present in the transformer and to ensure that they meet predefined requirements, a transformer with high harmonics is chosen. Nonlinear loads in offices or homes can result in harmonics in transformers. As a result, the distribution transformer, which has a very high economical value, may be harmed by the harmonics produced by this. For this reason, efforts are made to reduce the ensuing harmonics in order to preserve the transformer's longevity. In figure 6 the results of measurements of 11 transformers at ULP Syiah Kuala where there are transformers with high harmonics so it needs to be reduced can be seen that the THDi value of the transformer has passed the IEEE 159-2014 standard with a THDi standard limit of 10%, where the transformer is TKP 08- 00.

d. Distribution Transformer Loading Modelling

In order to ensure that the test conditions match the actual conditions, distribution transformer modeling attempts to match the simulated loading to the distribution transformer loading as measured by a measuring device. Modeling Distribution Systems with Simulink.

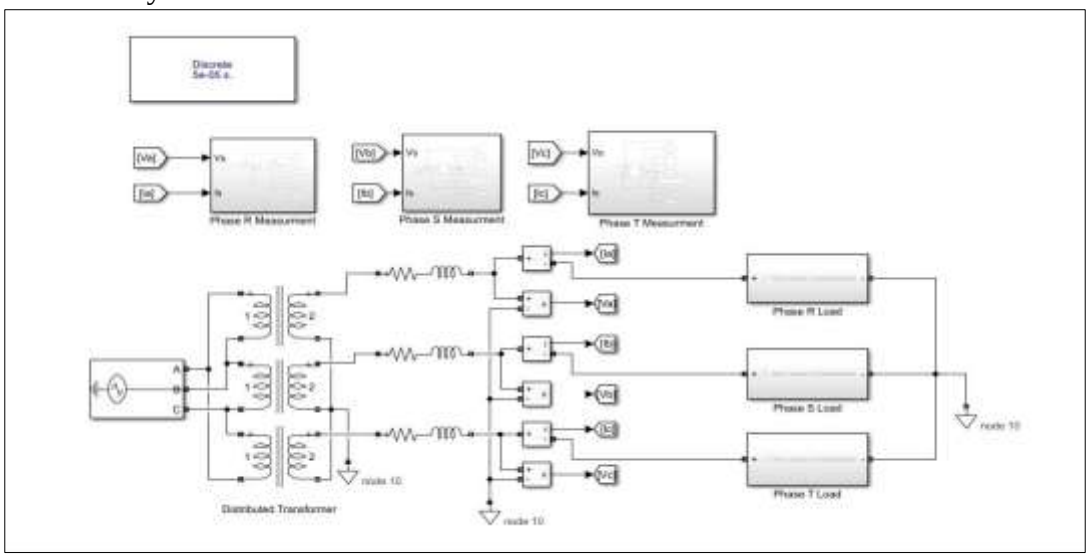

Figure 7. Distribution Channel Modeling

e. Mitigation Tool Modelling on Distribution Systems Using MATLAB

Furthermore, MATLAB software was used to develop a distribution system simulation model. The simulation's THDi, THDv, and harmonic order values will be compared to the measurement findings. Subsequently, a model of a passive filter is created and simulated, with the output results modeled in accordance with IEEE standard 519-2014. The following formula is used to perform the computation. Calculating Reactive Power Requirements.

$$Qc = P\{\tan(\cos^{-1} pf_1) - \tan(\cos^{-1} pf_2)$$

Where:

P = load

pf1 = initial power factor before repair

pf2 = initial power factor after repair

To meet these needs, a capacitive reactance is required of:

$$Xc = \frac{V^2}{Qc}$$

Passive Single-Tuned Filter Impedance Calculation:

$$C_f = \frac{1}{2\pi f . Xc}$$

Where:
L_f = Filter phase branch capacitance
F = Source frequency

Results and Discussion

The first test was conducted to observe battery charging, initiated at 09:00 and concluded at 09:45. Charging data is presented in Table 2, while the graphical representation of the charging progression can be observed in Figure 13.

Tabel 2. Measurement results

Time (hour)	Voltage (V)	Current (A)	Power (Watt)
09.00	3,32	0,0457	0,151724
09.05	3,36	0,0456	0,153216
09.10	3,42	0,0466	0,159372
09.15	3,43	0,0468	0,160524
09.20	3,46	0,0472	0,163312
09.25	3,67	0,0475	0,174325
09.30	3,75	0,0482	0,18075
09.35	3,78	0,0483	0,182574
09.40	3,95	0,0484	0,19118
09.45	4,22	0,0489	0,206358

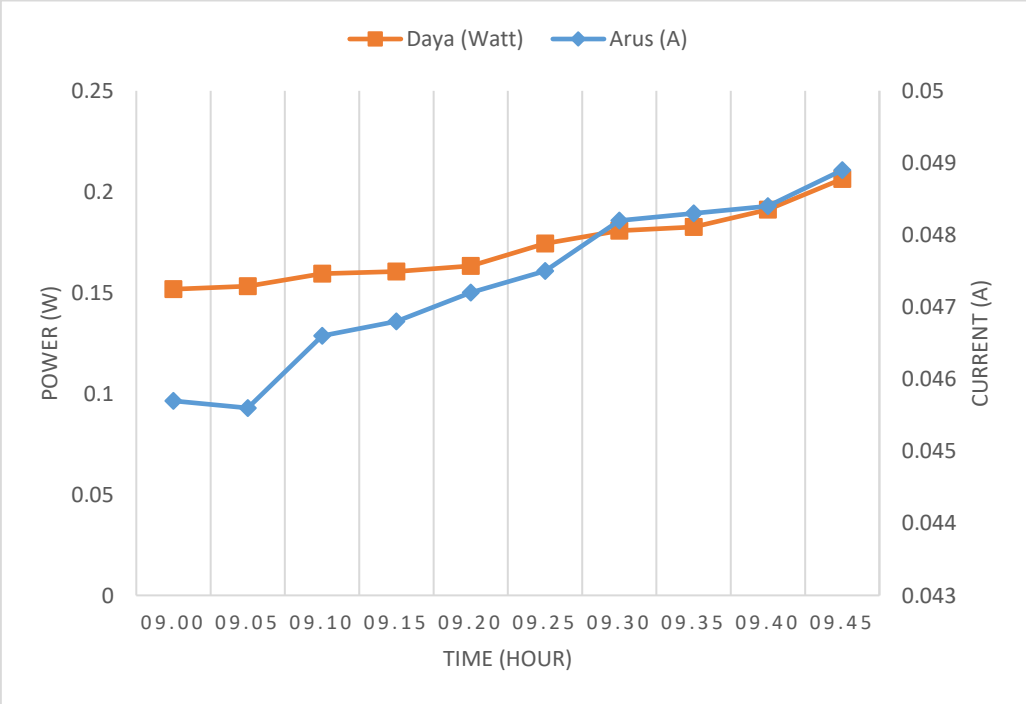

Figure 13. Power measurement graph during charging using solar panels

In Figure 13, it can be observed that the charging measurement was conducted using a mini solar panel connected to 3 Li-ION 18650 batteries arranged in parallel. The charging measurement commenced at 09:00 with an initial voltage of 3.32 V, current of 0.0457 A, resulting in a power output of 0.1517 watts. The charging process persisted until 09:45, spanning a duration of 45 minutes, reaching a voltage of 4.22 V, current of 0.048 A, and a generated power of 0.206358 watts. Consequently, the charging operation utilizing a mini solar panel with a voltage of 5 V and a current of 60mA was successfully executed and is deemed suitable for battery usage. The outcomes of this charging process can be employed to propel a warehouse robot. Figure 14 depicts the testing of the robot within the arena.

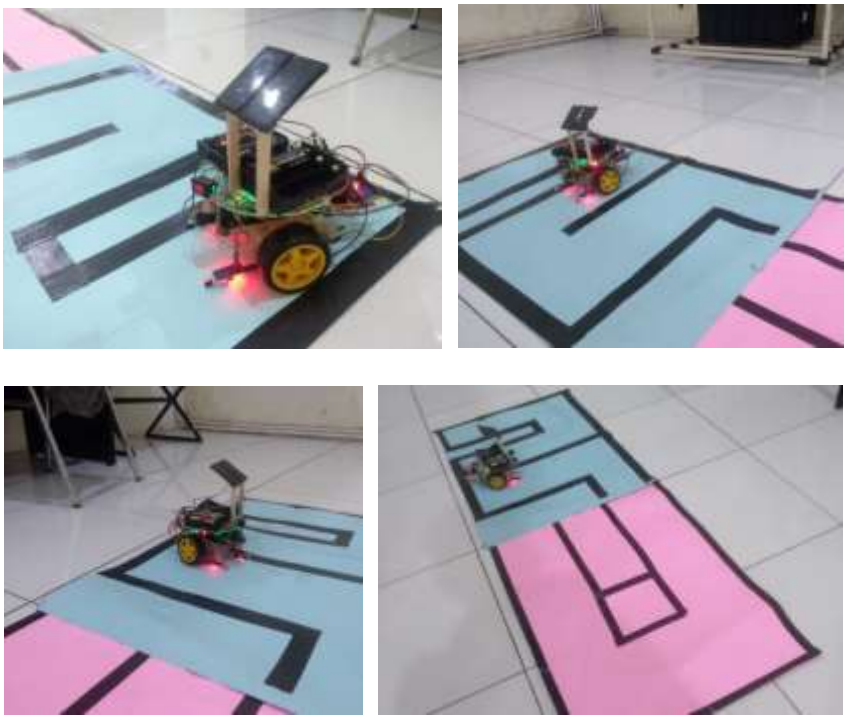

Figure 14. Robot Car Testing Process

The testing of the mobile robot commenced with the measurement of the power charged through a solar panel with a capacity of 2.06358 watts and a voltage of 4.22 V. Assembled in series to facilitate the propulsion of the mobile robot, the resultant voltage was 12.66. The testing initiative was initiated at 10:15 AM Western Indonesian Time (WIB), and the pertinent test data is elucidated in Table 3.

Table 3. Rotational Performance of the Robot Car

Time (hour)	n^{th} rotation	Output voltage (V)	Status
10.15	0	12,35	Normal
10.18	1	11,68	Normal
10.21	2	11,01	Normal
10.24	3	10,34	Normal
10.27	4	9,67	Normal
10.30	5	9	Slowing down
10.33	6	8,33	Slowing down
10.36	7	7,66	Slowing down

10.39	8	6,99	Stop

Table 3 illustrates that the testing of the robotic car commenced from 10:15 to 10:39. The robotic vehicle operated for a duration of 29 minutes. During the first to the fourth rounds, the performance of the robot car was flawless, aligning with the pre-programmed specifications, with a voltage range from 12.35 volts to 9.67 volts. In the fifth round to the seventh round of testing, the robotic vehicle began to decelerate, exhibiting voltages ranging from 9 volts to 7.66 volts. Finally, the robot came to a halt in the eighth round, registering a voltage of 6.99 volts.

Following the robot car testing, the subsequent step involved acquiring data on the voltage output measurements concerning the power generated by the robot during its 29-minute operation, utilizing the ACS172 current sensor. Table 4 presents the output data from the initial round to the eighth round. Figure 15 depicts the power consumption graph.

Table 4. The output power data for the robot car

Time (hour)	Output voltage(V)	current (A)	Power (Watt)
10.15	12,35	0,0502	0,61997
10.18	11,68	0,0482	0,562976
10.21	11,01	0,04725	0,5202225
10.24	10,34	0,0442	0,457028
10.27	9,67	0,0432	0,417744
10.30	9	0,04213	0,37917
10.33	8,33	0,0325	0,270725
10.36	7,66	0,0315	0,24129
10.39	6,99	0,0287	0,200613

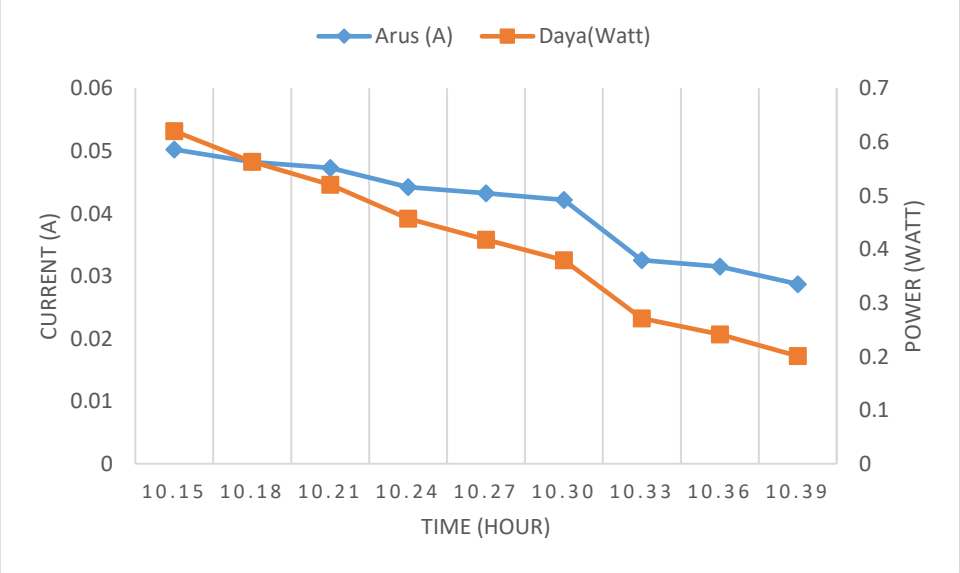

Figure 15. Power Consumption Graph of Robot Car

In Figure 15, it is observed that the current and power of the mobile robot consistently decrease throughout each test. During the 8-round, 29-minute trial, the lowest recorded current was 0.0287 A, and the corresponding power was 0.206 watts. Subsequently, an efficiency calculation for charging using solar panels was conducted.

Before performing the efficiency calculation, it is essential to have the specifications of the solar panel and the battery output that powers the mobile robot. Table 5 presents the specification data and the average measurement results.

Table 5. Specification Data and Measurement Results of Solar Panel and Battery

Specification		
Name	**Current(A)**	**Voltage(V)**
Solar Panel	0.065	4.8
Battery	0.058	11.1
Measurement results		
Name	**Current(A)**	**Voltage(V)**
Solar Panel	0.0473	3.36
Battery	0,0408	9,67

From the data in Table 5, calculations were performed using (4). Subsequently, the Fill Factor for the solar panel was determined

$$FF = \frac{Vpm \times Ipm}{Voc \times Isc}$$

$$FFsolarpanel = \frac{3.36\ \text{V} \times 0.0473\ \text{A}}{4.8\ \text{V} \times 0.065\ \text{A}} = 0{,}55146$$

Next, the Fill Factor calculation for the Li-Ion battery during its usage was carried out using (4).

$$FF = \frac{Vpm \times Ipm}{Voc \times Isc}$$

$$FF = \frac{9{,}67\ V \times 0{,}0408\ \text{A}}{11.1 \times 0.058\ \text{A}} = 0{,}613959$$

Subsequently, calculating P solar Panel and P Battery, namely:

$$Psolar = 4.8 \times 0.065 \times 0{,}55146 = 0{,}17205552\ W$$
$$Pbaterai = 11.1 \times 0.058 \times 0{,}613958717 = 0{,}395266622\ W$$

By employing (3), the efficiency calculation of power concerning the solar panel and battery usage can be determined as:

$$P\% = \frac{P_{solar}}{Pbaterai} \times 100\%$$

$$P\% = \frac{0.1720\ W}{0.3952\ W} \times 100\% = 43{,}5\%$$

In accordance with the measurement results during the charging of the Li-Ion battery by the solar panel and the performance testing of the mobile robot, the obtained efficiency of Li-Ion battery charging is 43.5%. The findings of this study regarding the energy consumption of the battery in relation to the mobile robot are also consistent with the results of a study titled "Experimental analysis on solar-powered mobile robot as the prototype for environmentally friendly automated transportation." In that study, the utilization of solar panel energy to drive the mobile robot was explained, with a voltage capacity of 5.2 V, facilitated by the use of a capacitor to increase the voltage to 12.64 V. The charging process in that study spanned 5 days to mobilize the robot [2]. The novelty of this research lies in analyzing miniature solar panels used to charge Li-

Ion batteries with a voltage of 3.3 V, comprising three batteries charged in parallel for 45 minutes, and at a voltage of 11.1 V when connected in series for 29 minutes.

Conclusion

This research examines the utilization of mini solar panels and the application of three Li-ION 18650 3.3V batteries in a mini mobile robot employed in a warehouse setting. The battery recharging in this study was successfully accomplished using mini solar panels connected through a solar control mechanism. The specifications of the employed solar panels include a voltage of 5V and a current of 60mA. Two solar panels were installed, resulting in a maximum power output of 0.206358 watts. The charging duration to full capacity was observed to be 45 minutes. The robot's performance was evaluated in an arena with dimensions of 80 cm x 50 cm, revealing that the robot could complete 8 rotations with a travel time of 29 minutes.

The assessment of power and output voltage was conducted based on readings from the ACS172 current sensor. It was identified that the system generated a minimum current of 0.0287 A, with a remaining battery power of 0.200613 watts. The efficiency test of the robot's performance concerning battery charging using mini solar panels yielded a 43.5% efficiency rate. Recommendations arising from this study emphasize the development of solar panels to continually enhance battery energy efficiency, thereby extending usage time and reducing charging duration. Furthermore, the integration of the solar panel energy system into the robot is envisioned to be applicable on a larger scale.

References

[1] A. Hassan, R. M. Asif, A. U. Rehman, Z. Nishtar, M. K. A. Kaabar, and K. Afsar, “Design and Development of an Irrigation Mobile Robot,” *IAES Int. J. Robot. Autom. (IJRA,* vol. 10, no. 2, doi: 10.11591/ijra.v10i2.pp75-90.

[2] T. Dewi, P. Risma, Y. Oktarina, A. Taqwa, Rusdianasari, and H. Renaldi, “Experimental Analysis on Solar Powered Mobile Robot as the Prototype for Environmentally Friendly Automated Transportation,” *J. Phys. Conf. Ser.*, vol. 1450, no. 1, doi: 10.1088/1742-6596/1450/1/012034.

[3] P. Nattharith and T. Kosum, “Development of Mobile Robot System for Monitoring and Cleaning of Solar Panels,” *GMSARN Int. J.*, vol. 16, no. 3, pp. 302–6.

[4] A. Chellal, J. Lima, A. I. Pereira, and P. Costa, “Innovative Robot Design for Cleaning Solar Panels,” in *Proceedings of the 11th International Conference on Simulation and Modeling Methodologies, Technologies and Applications, SIMULTECH 2021*, doi: 10.5220/0010540102640270.

[5] T. Sorndach, N. Pudchuen, and P. Srisungsitthisunti, “Rooftop Solar Panel Cleaning Robot Using Omni Wheels,” in *2018 2nd International Conference on Engineering Innovation, ICEI 2018*, pp. 7–12. doi: 10.1109/ICEI18.2018.8448530.

[6] R. A. Nanda, A. Supriyanto, F. M. Dewadi, R. R. Jati, and L. A. Kurniawan, “Perancangan Dan Perakitan Elektronika Mikrokontroler Berbasis Iot Untuk Studi Pengukuran Sistem Hvac (Design and Assembly of IoT-Based Microcontroller Electronics for HVAC System Measurement Studies),” *Buana Ilmu*, vol. 7, no. 1, pp. 43–55, 2022.

[7] R. Hasrul, “Sistem Pendinginan Aktif Versus Pasif Di Meningkatkan Output Panel Surya (Active Cooling System Versus Passive in Enhancing Solar Panel

Output)," *J. Sain, Energi, Teknol. Ind.*, vol. 5, no. 2, pp. 79–87.
[8] R. A. Nanda, A. Supriyanto, and F. M. Dewadi, "Using the MPX5500DP Sensor for Monitoring Microcontroller-Based HVAC Systems and IOT," *REM (Rekayasa Energi Manufaktur) J.*, vol. 8, no. 1, pp. 1–8.
[9] R. A. Nanda, A. Arhami, and R. Kurniawan, "Perancangan Dan Pengujian Model Mobil Robot Penanam Bibit Kangkung (Design and Testing of a Robot Model for Planting Water Spinach Seeds)," *Rona Tek. Pertan.*, vol. 13, no. 2, pp. 14–28.
[10] B. Bat-Erdene and O. E. Mandakh, "Shepherding Algorithm of Multi-Mobile Robot System," in *Proceedings - 2017 1st IEEE International Conference on Robotic Computing, IRC 2017*, pp. 358–61. doi: 10.1109/IRC.2017.51.
[11] T. G. Thuruthel, E. Falotico, M. Cianchetti, and C. Laschi, "Design of a Tendon-Drive Manipulator for Positioning a Probe of a Cooperative Robot System for Fault Diagnosis of Solar Panels at Mega Solar Power Plant," *CISM Int. Cent. Mech. Sci.*, vol. 569, no. January, pp. 47–54, doi: 10.1007/978-3-319-33714-2.
[12] F. Septiarini, T. Dewi, and R. Rusdianasari, "Fuzzy Logic Controller Application for Automatic Charging System Design of a Solar Powered Mobile Manipulator," *Comput. Eng. Appl. J.*, vol. 10, no. 3, pp. 137–50, doi: 10.18495/comengapp.v10i3.380.
[13] J. Cruz-Lambert *et al.*, "Converter Design for Solar Powered Outdoor Mobile Robot," in *World Automation Congress Proceedings 2016-Octob:1–6*, doi: 10.1109/WAC.2016.7583016.
[14] N. Ronnaronglit and N. Maneerat, "A Cleaning Robot for Solar Panels," in *Proceeding - 5th International Conference on Engineering, Applied Sciences and Technology, ICEAST 2019*, pp. 1–4. doi: 10.1109/ICEAST.2019.8802521.
[15] I. Arissetyadhi, T. Dewi, and R. D. Kusumanto, "Experimental Study on The Effect of Arches Setting on Semi-Flexible Monocrystalline Solar Panels," in *Kinetik: Game Technology, Information System, Computer Network, Computing, Electronics, and Control (May):111–18*. doi: 10.22219/kinetik.v5i2.1055.
[16] P. A. Plonski, J. Vander Hook, and V. Isler, "Environment and Solar Map Construction for Solar-Powered Mobile Systems," *IEEE Trans. Robot.*, vol. 32, no. 1, pp. 70–82, doi: 10.1109/TRO.2015.2501924.
[17] A. N. R. Arhami and K. Rudi, "Structural Analysis of Mobile Robot Frame for Spinach Water Seed Planting Using Finite Element Method," in *Pp. 177–86 in Proceedings of the 3rd International Conference on Experimental and Computational Mechanics in Engineering: ICECME 2021*, Banda Aceh: Springer Nature Singapore Singapore.
[18] P. Zarafshan and S. A. A. Moosavian, "Adaptive Hybrid Suppression Control of a Wheeled Mobile Robot with Active Flexible Members," in *2011 IEEE International Conference on Mechatronics and Automation, ICMA 2011*, pp. 932–37. doi: 10.1109/ICMA.2011.5985715.